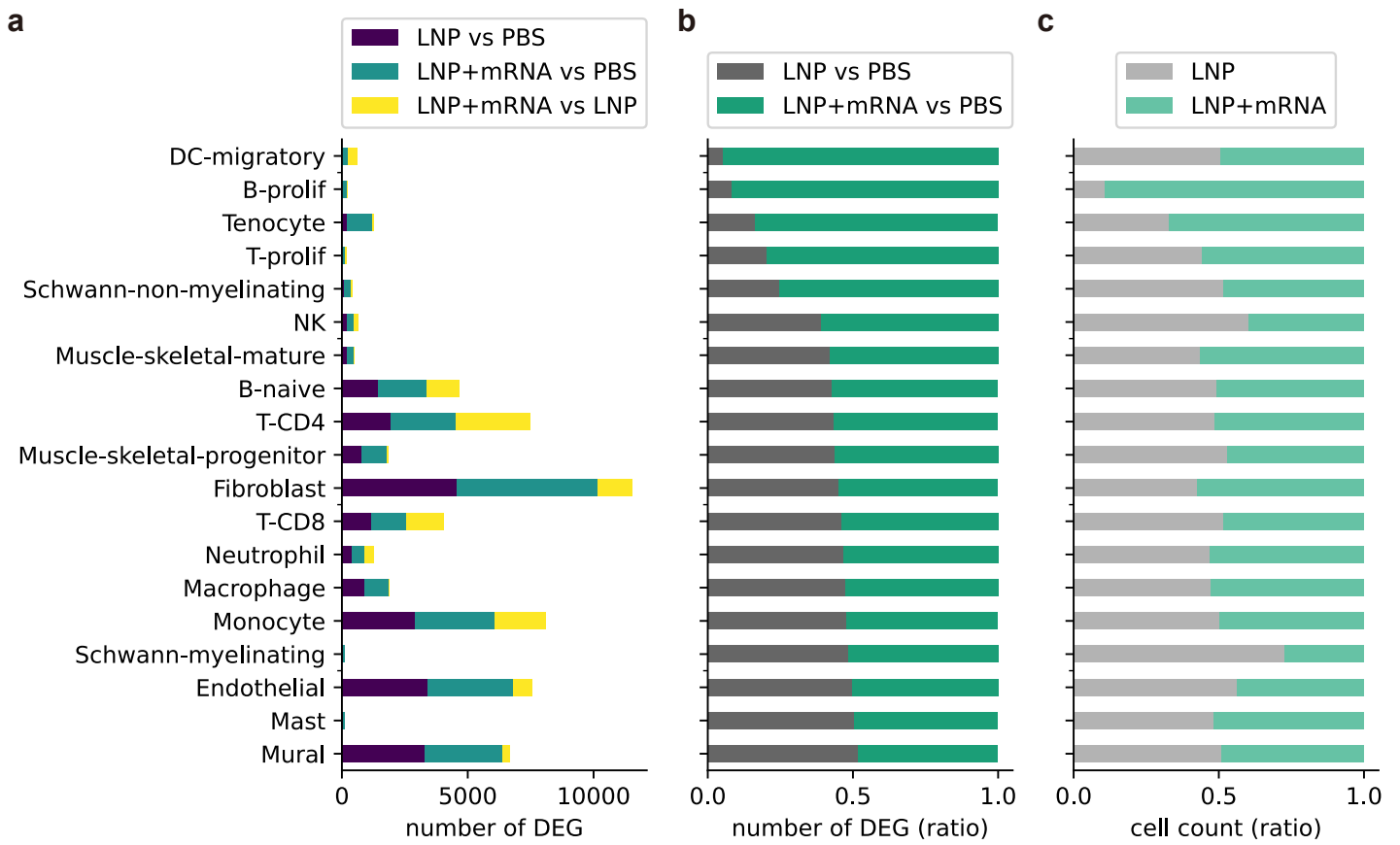
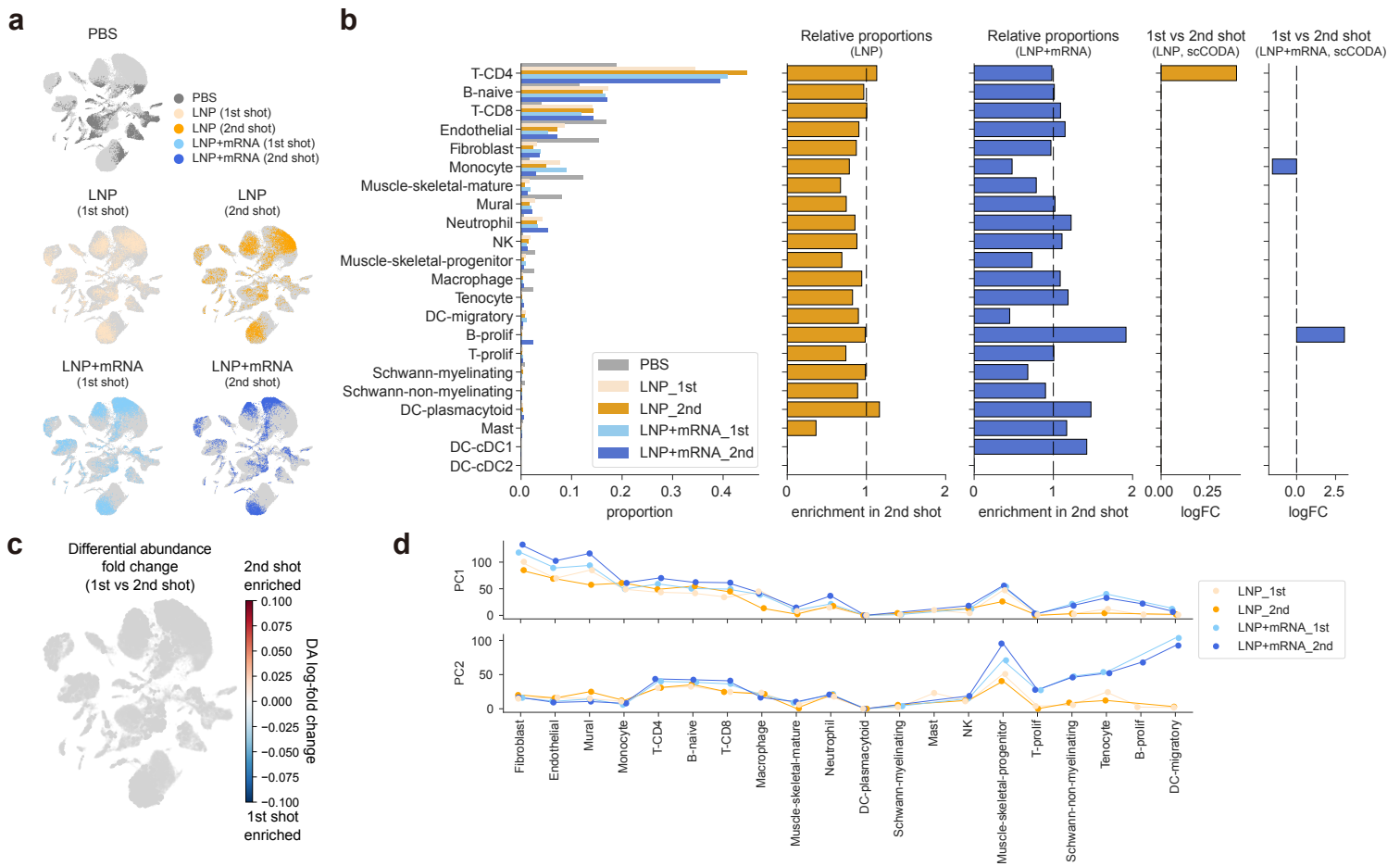


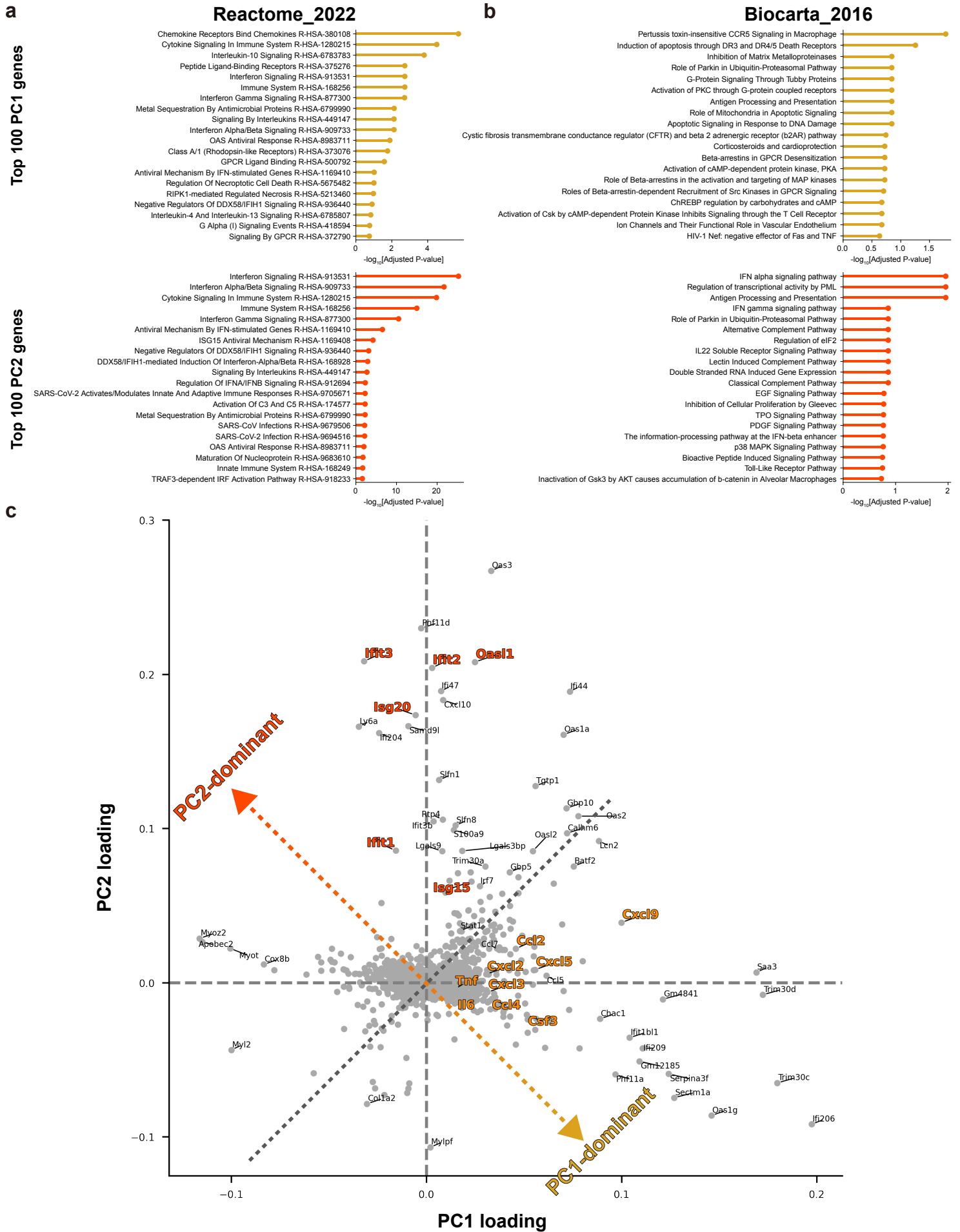
Supplementary Fig. 1. Automated electrophoresis results of in vitro-transcribed (IVT) mRNA used in this study. **a,b,** (a) Gel images and (b) electropherogram of IVT mRNA are shown with size indicators.



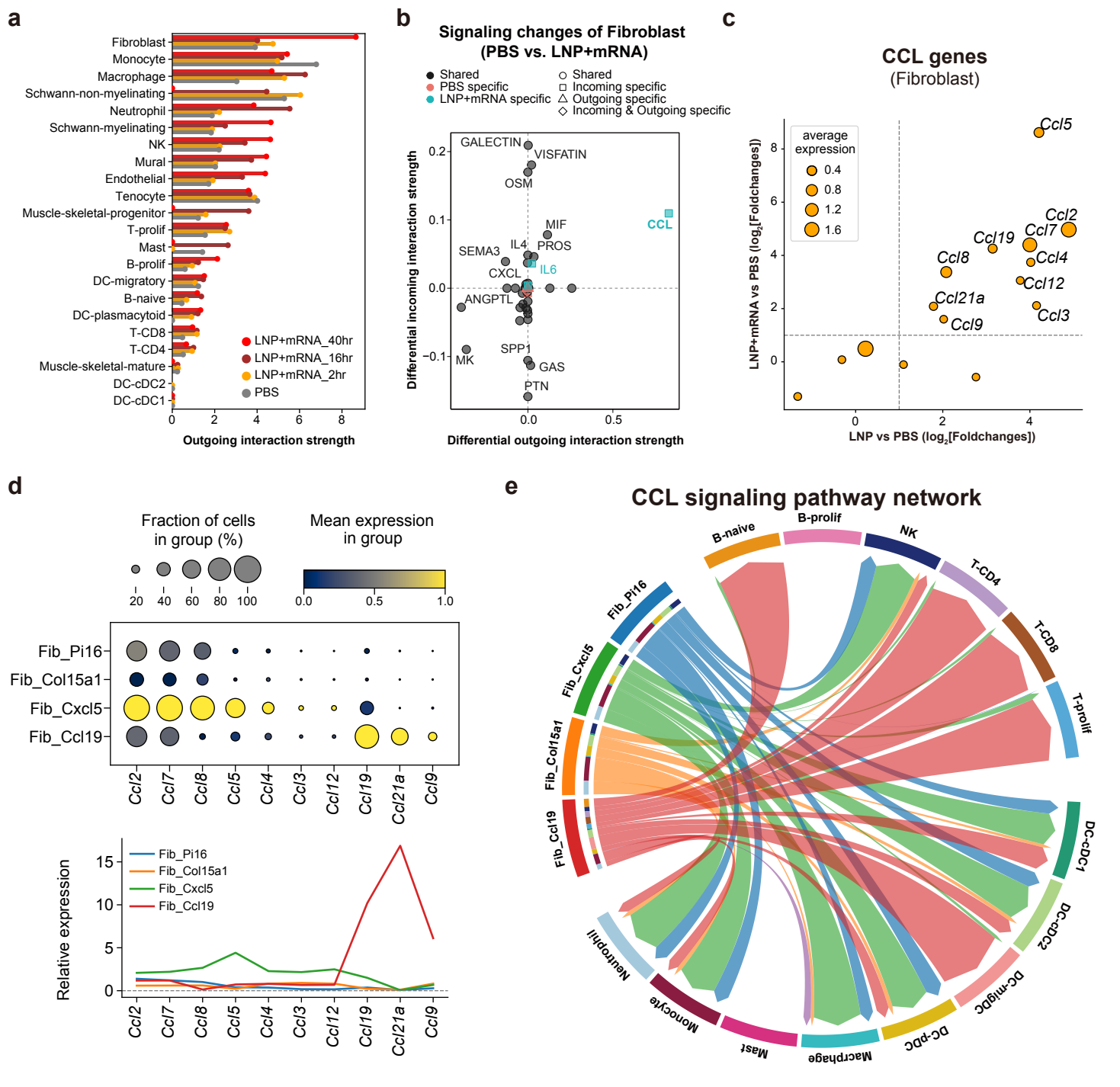
Supplementary Fig. 2. Number of differentially expressed genes according to the cell types and conditions. **a**, Bar plot showing the number of differentially expressed genes (DEGs) between 16 h post injection (p.i.) samples of PBS, LNP, and LNP+mRNA. **b**, Bar plot showing the ratio of DEG counts between LNP (vs PBS) and LNP+mRNA (vs PBS) (middle). **c**, Ratio of cell counts in each treatment condition is shown in the bar plot.



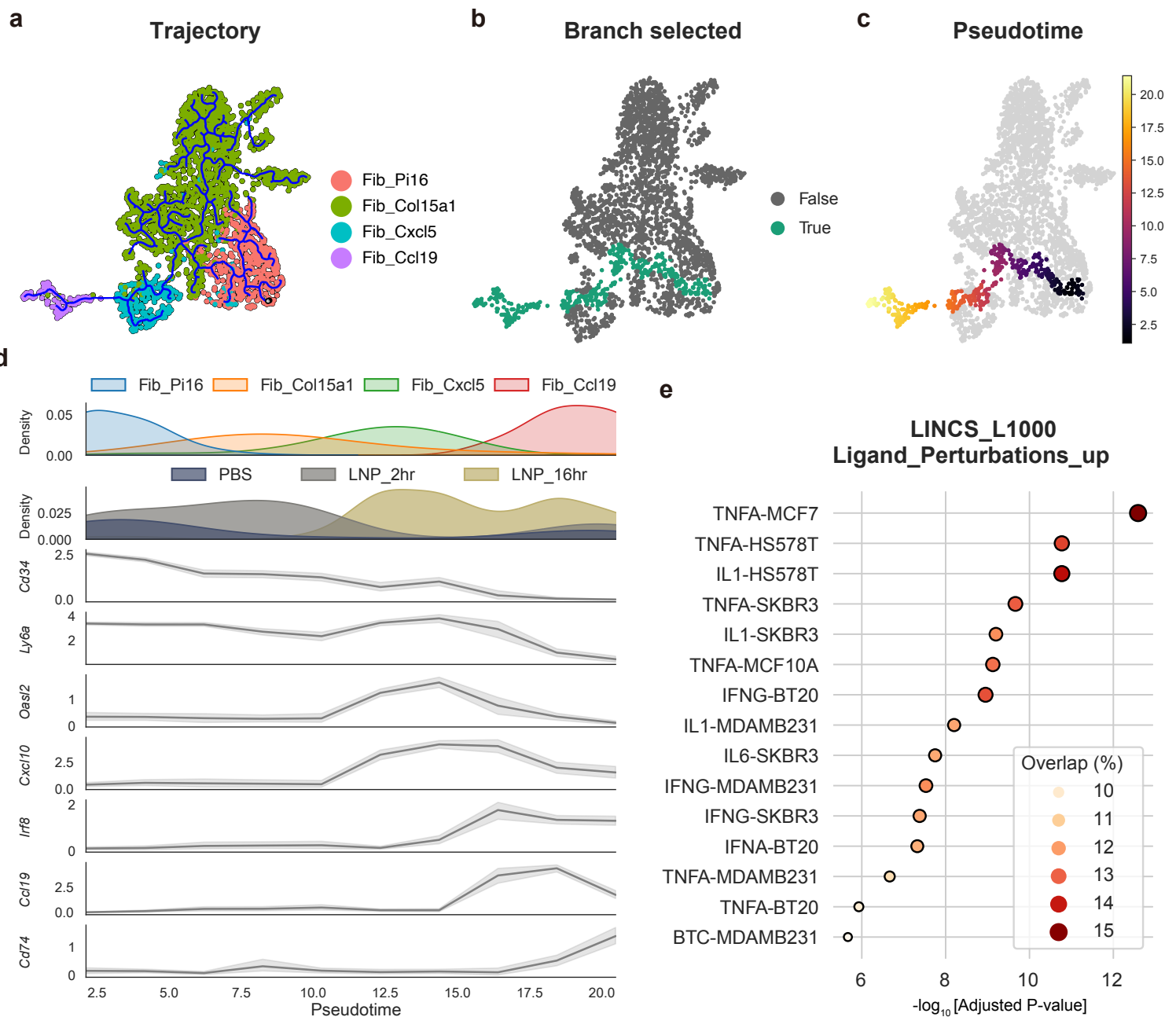
Supplementary Fig. 3. Comparing initial responses to prime and boost shots of the vaccine at 16 h p.i. time point.
a, Primary and boost shot samples are displayed on the UMAP landscape of single-cell transcriptome data. Colors indicate injection type and number of shots given. **b**, Cell compositions in primary and boost shot samples. Bar plots showing (left) raw proportion of cell types in the primary and boost shot samples, (middle) relative proportions, indicating cell type proportions in the boost shot condition divided by the average proportions in the primary and boost shot, and (right) log-fold changes of cellular composition, which is determined by differential cell composition analysis (false discovery rate < 0.05). **c**, The result from differential abundance testing is displayed on the UMAP landscape. Colors indicate log-fold changes between 1st and 2nd shots of LNP and LNP+mRNA injections. **d**, Line plots showing the PC projections of cell type-wise DEG vectors, which is acquired by the systematic comparison with cells in PBS sample.



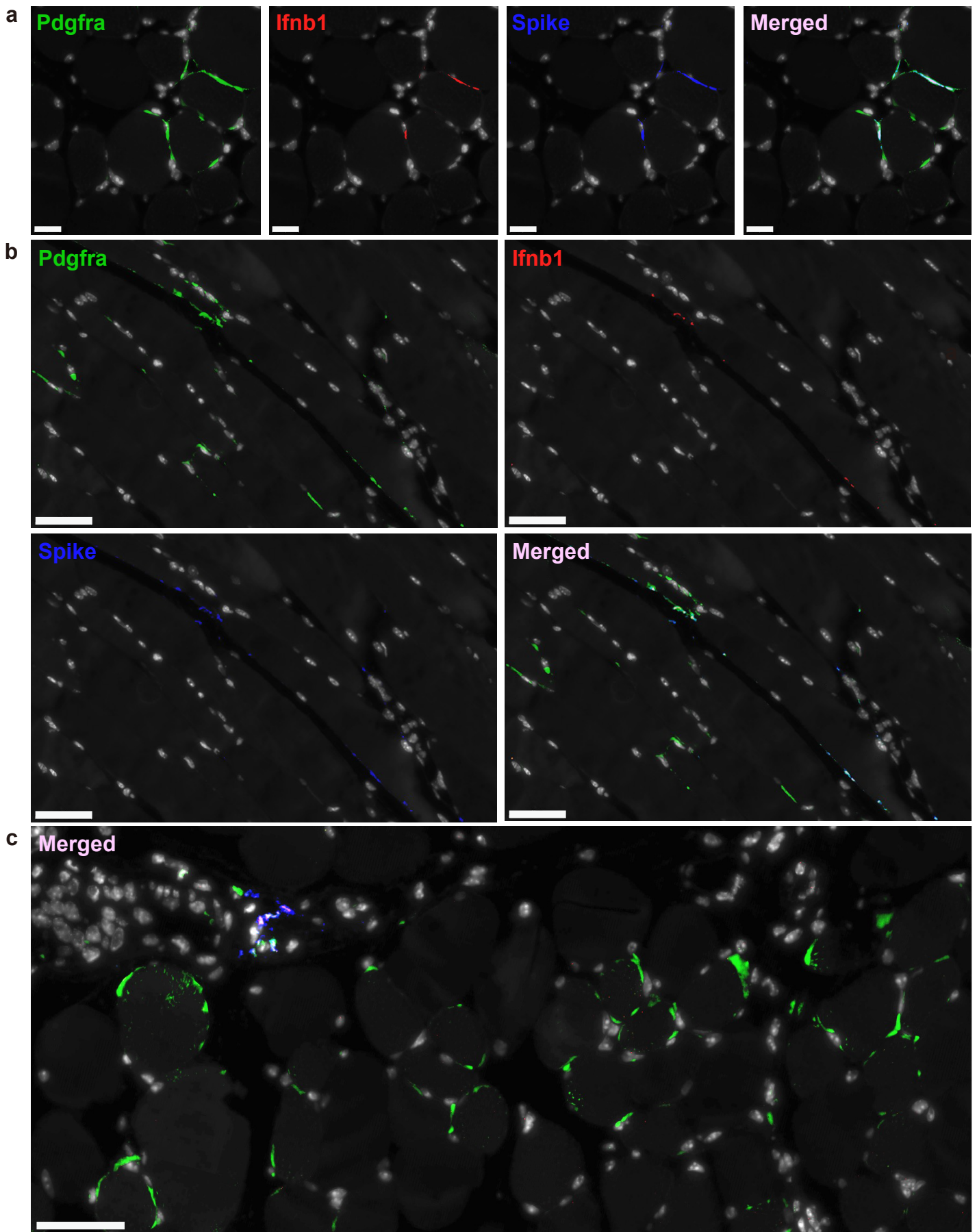
Supplementary Fig. 4. PC1- and PC2-associated genes. **a,b**, Results from pathway enrichment analysis using terms from **(a)** Reactome_2022 and **(b)** Biocarta_2016, on the top 100 PC1 genes (top panels) and top 100 PC2 genes (bottom panels), according to the coefficients to the PC axes. **c**, Scatter plot showing the coefficients of individual genes to the PC1 (x-axis) and PC2 axes (y-axis).



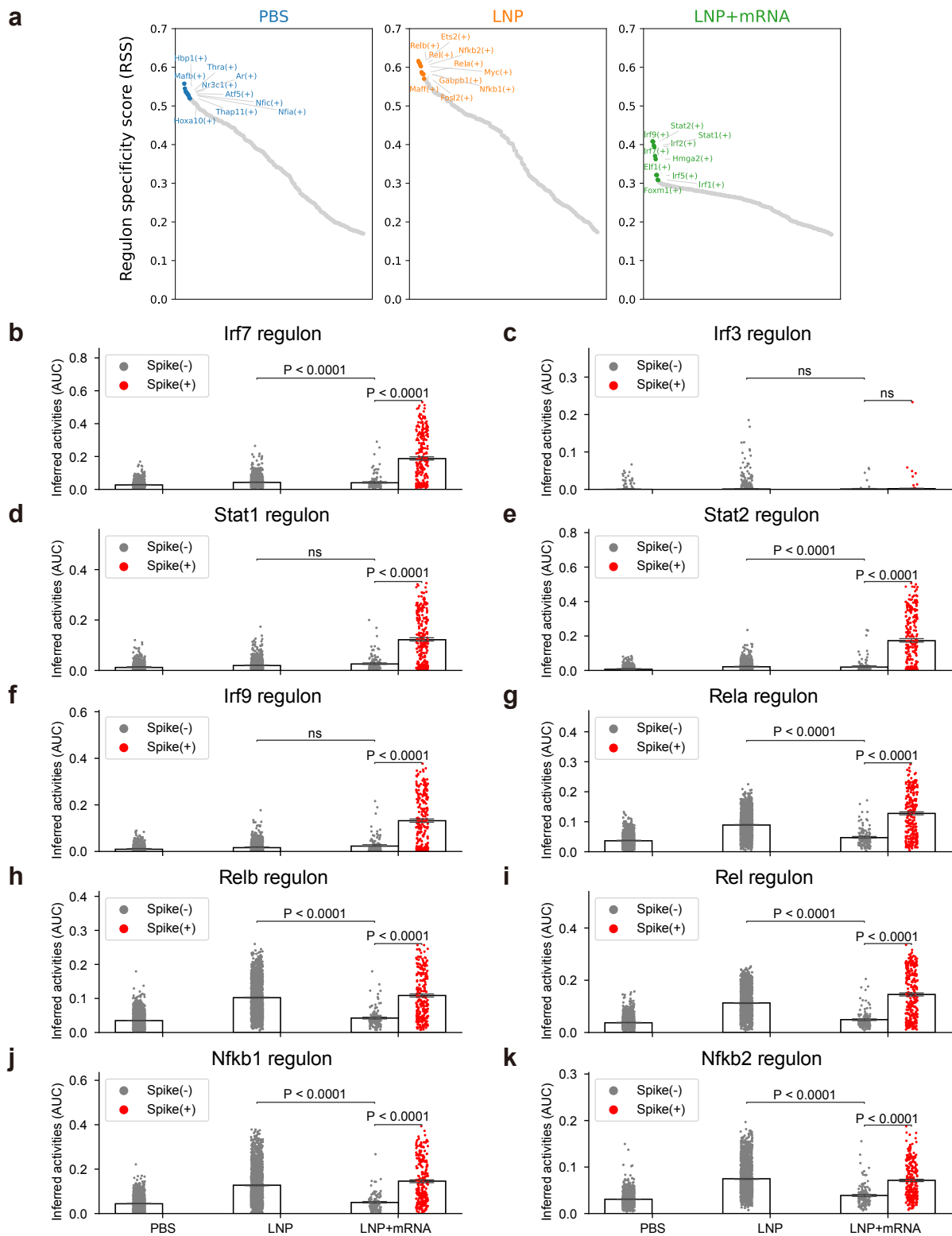
Supplementary Fig. 5. Injection-site fibroblasts express chemokine genes in response to mRNA vaccine. **a**, Outgoing signaling strengths of cell types at each p.i. time point after mRNA vaccine injection. Signaling strengths were inferred from the injection-site scRNA-seq data using CellChat. **b**, Differential cellular signaling patterns in the injection-site fibroblasts. Fibroblasts from the mRNA vaccine injection and PBS injection were compared using CellChat, and the positive values on the x-axis and the y-axis indicate higher signaling with the mRNA vaccine injection. **c**, Scatter plot showing induction of CCL (CC chemokine ligand) genes. Fibroblasts from PBS-injected, LNP-injected, and LNP+mRNA (mRNA vaccine)-injected scRNA-seq data were compared. The x-axis of the scatter plot indicates \log_2 fold changes for LNP-treated fibroblasts (vs PBS), and the y-axis denotes \log_2 fold changes of LNP+mRNA fibroblasts (vs PBS). Sizes indicate average expression of the genes in fibroblasts. **d**, Differential expression of CCL genes according to fibroblast population identities depicted as a dot plot (top) and a line plot (bottom). Dot sizes in the dot plot represent fractions of cells expressing genes, and colors indicate min-max scaled average expression of the genes. The y-axis on the line plot represents relative average expression (vs average expression in total fibroblasts) of the genes. **e**, A chord plot representation of the CCL signaling network inferred from the injection-site scRNA-seq data using CellChat.



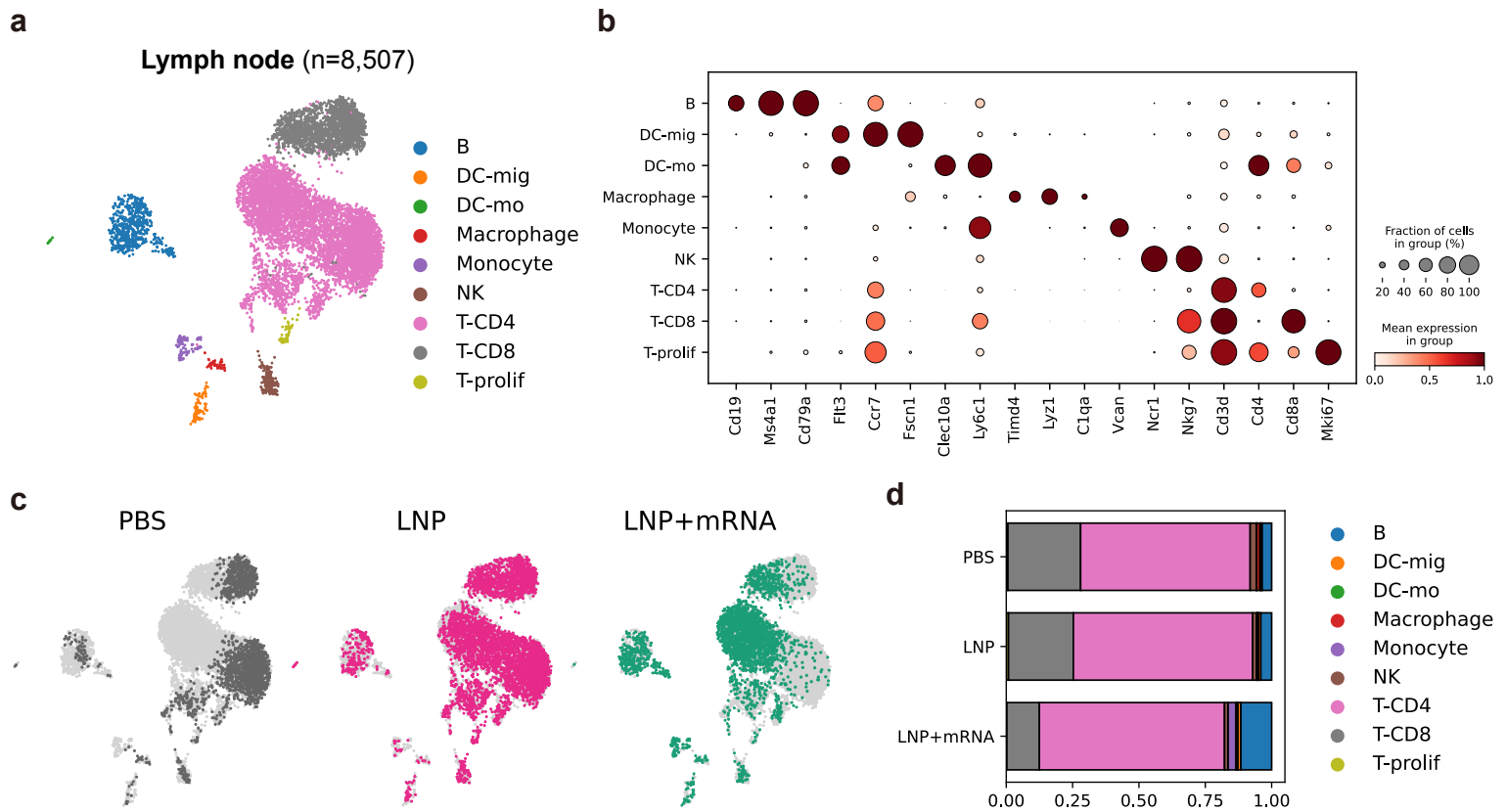
Supplementary Fig. 6. Trajectory analysis on injection-site fibroblasts after LNP injection. **a-c**, Results from single-cell trajectory analysis. **(a)** Whole trajectory graphs, **(b)** a selected trajectory branch that spans from Fib_Pi16 to Fib_Ccl19, and **(c)** calculated pseudotimes are displayed on the UMAP representation of LNP-treated injection-site fibroblasts. **d**, Fibroblasts on the selected branch (as in **b**) are aligned according to trajectory pseudotime (as in **c**), and their cellular identities, treatment conditions, and expression of genes highly associated with Ccl19+ fibroblast identity are displayed as line plots. Line plots indicate average expression and the error bands indicate 95% confidence intervals. **e**, Pathway enrichment analysis on the pseudotime correlated genes, defined as the genes with Pearson correlation coefficients > 0.3 to the pseudotime values across the fibroblasts on the selected branch. *P* values were adjusted with the Benjamini-Hochberg method.



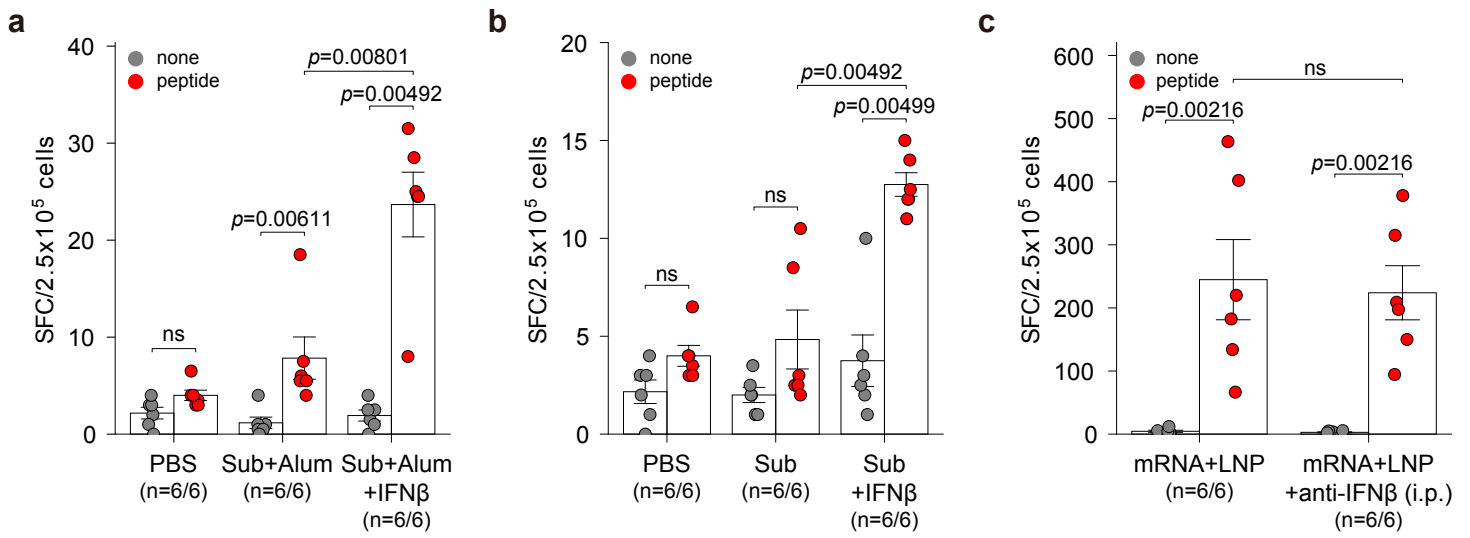
Supplementary Fig. 7. RNA in situ hybridization reveals spike-specific induction of *Ifnb1* in fibroblasts. a-c, RNA in situ hybridization was performed on the 2 h mRNA vaccine p.i. muscle tissues (injection site) with detection probes for *Pdgfra* (green), *Ifnb1* (red), and Spike (blue) transcripts. Fluorescent images were taken at various scales. Scale bars (white bar at the lower left corner) indicate (a) 20 μm and (b-c) 50 μm. Images were selected from biological replicates of mRNA-vaccine injected samples (n=4).



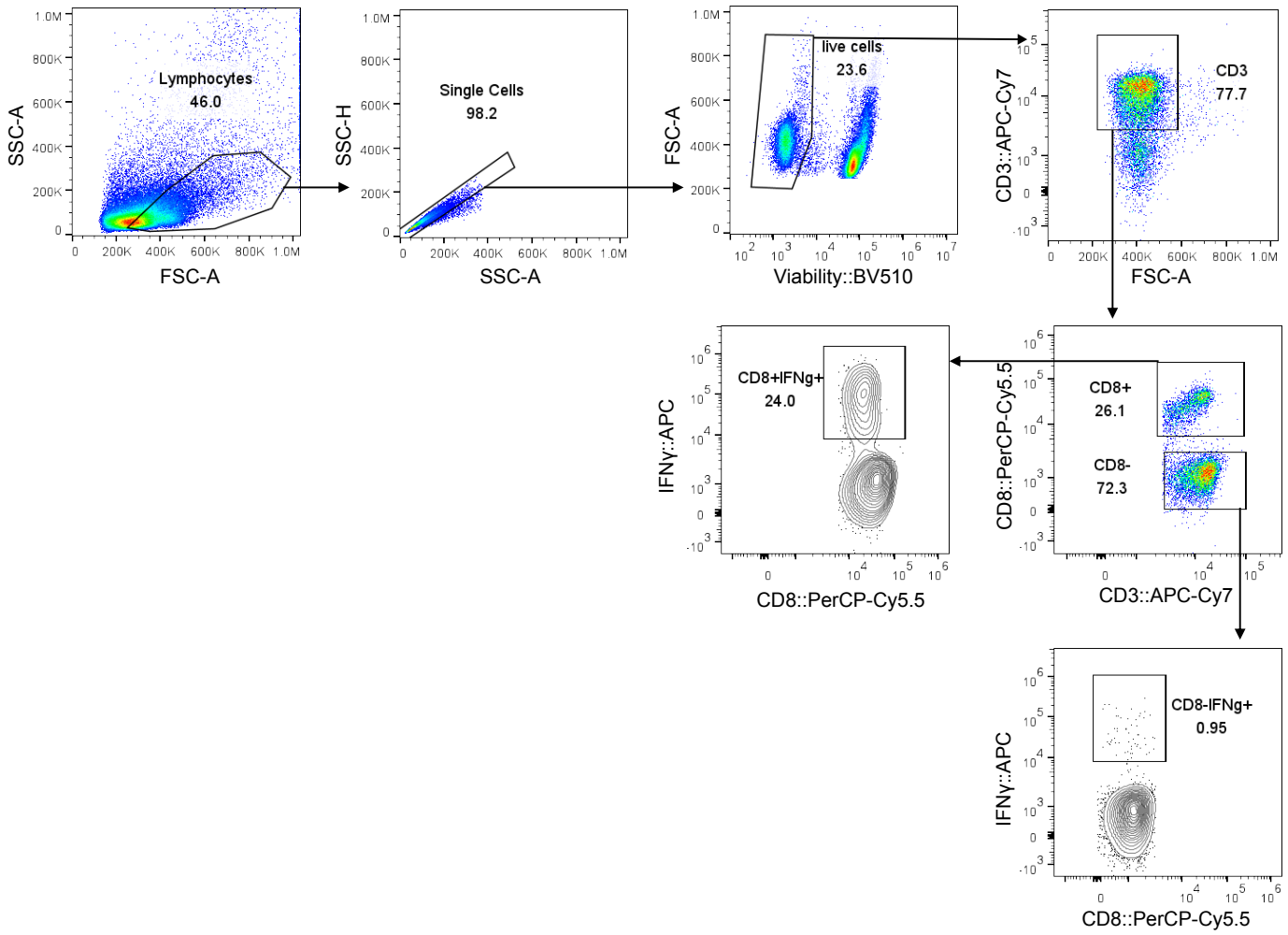
Supplementary Fig. 8. Gene regulatory network analysis on the 2 h p.i. fibroblasts. **a**, Differential regulon activities identified in gene regulatory network analysis. **b-k**, Regulon activities in individual fibroblasts from PBS injection, LNP 2 h p.i., and LNP+mRNA 2 h p.i. samples are displayed in bar plots. Colors indicate detection of spike mRNA in each fibroblast. Statistical comparison between the groups were conducted with two-tailed MannWhitney U tests (ns: non-significant). All the data in bar plots are presented as mean values +/- SEM.



Supplementary Fig. 9. Draining lymph node single-cell transcriptome data. **a**, UMAP representation of cell types in the draining lymph node scRNA-seq data. **b**, Representative marker genes and their expression in the cell types identified in scRNA-seq data. Dot sizes are proportional to the expressing cell ratio, and the colors indicate min-max normalized average expression values of the marker genes. **c**, The cells from each treatment condition are separately displayed on the UMAP. **d**, Cell type compositions in scRNA-seq data from each of the treatment conditions. Colors indicate cell type identities (as in **a**).



Supplementary Fig. 10. Intramuscular IFN- β promotes cellular immune responses. a-c, Results from the IFN- γ ELISpot assay conducted on splenocytes from various conditions are displayed on bar plots. The effect of IFN- β co-injection was evaluated on each vaccination strategy: (a) protein subunit+Alum, (b) protein subunit. The effect of non-injection site IFN- β blocking was evaluated in (c) mRNA+LNP (i.m.) with or without IFN- β blocking antibody (i.p.). Cells were stimulated with spike peptide (red) or not (gray), and the spot counts were statistically evaluated with two-tailed MannWhitney U tests (ns: non-significant). All the data in bar plots are presented as mean values +/- SEM.



Supplementary Fig. 11. Gating strategy to analyze IFN- γ producing T-cells in vaccinated mice spleen. Splenocytes were isolated from mice by mechanical disruption on a 40 μ m cell strainer. Lymphocytes were first gated using FSC-A and SSC-A, doublets were sequentially excluded by combining SSC-A and SSC-H. Cells were labeled with viability dye to exclude dead cells, and with anti-CD3, -CD8 antibodies followed by fixation and permeabilization and then stained with anti-IFN- γ . IFN- γ producing T-cells were defined as CD3+CD8+IFN- γ + or CD3+CD8-IFN- γ + cells.